PHYSICAL REVIEW B **78**, 035101 (2008)

Effect of static and dynamic disorder on electronic transport in RCo$_2$ compounds: Ho(Al$_x$Co$_{1-x}$)$_2$ alloys

A. T. Burkov
A. F. Ioffe Physico-Technical Institute, Russian Academy of Sciences, Sankt-Petersburg 194021, Russia

E. Bauer and E. Gratz
Institute of Experimental Physics, Vienna Technical University, Wiedner Hauptstrasse 8-10, A-1040 Vienna, Austria

R. Resel
Institute of Solid State Physics, Graz University of Technology, Petergasse 16, A-8010 Graz, Austria

T. Nakama and K. Yagasaki
Department of Physics, College of Science, University of the Ryukyus, Okinawa 903-0213, Japan

(Received 28 March 2008; published 1 July 2008)

We present experimental results on thermoelectric power (S) and electrical resistivity (ρ) of pseudobinary alloys Ho(Al$_x$Co$_{1-x}$)$_2$ ($0 \leq x \leq 0.1$), in the temperature range 4.2 to 300 K. The work focuses on the effects of static (induced by alloying) and dynamic (induced by temperature) disorder on the magnetic state and electronic transport in a metallic system with itinerant metamagnetic instability. Spatial fluctuations of the local magnetic susceptibility in the alloys lead to the development of a partially-ordered magnetic ground state of the itinerant 3d electron system. This results in a strong increase of the residual resistivity and a suppression of the temperature-dependent resistivity. Thermopower exhibits a complex temperature variation in both the magnetically ordered and in the paramagnetic state. This complex temperature variation is attributed to the electronic density-of-states features in vicinity of Fermi energy and to the interplay of magnetic and impurity scattering. Our results indicate that the magnetic enhancement of the Co 3d band in RCo$_2$-based alloys upon a substitution of Co by nonmagnetic elements is mainly related to a progressive localization of the Co 3d electrons caused by disorder. We show that the magnitude of the resistivity jump at the Curie temperature for RCo$_2$ compounds exhibiting a first-order phase transition is a nonmonotonic function of the Curie temperature due to a saturation of the 3d-band spin-fluctuation magnitude at high temperatures.

DOI: 10.1103/PhysRevB.78.035101 PACS number(s): 71.27.+a, 72.15.Gd, 72.15.Jf, 75.10.Lp

HoCo$_2$ belongs to the family of intermetallic RCo$_2$ cubic Laves phases (R stands for rare-earth elements) which are well known for their outstanding magnetic properties associated with itinerant 3d electron subsystem.[1–3] Long-range magnetic order of the 3d electron subsystem of paramagnetic YCo$_2$ and LuCo$_2$ can be induced by external magnetic field exceeding a certain critical value B_c. This critical field was found to be about 70 T for YCo$_2$ (Ref. 4) and about 77 T for LuCo$_2$.[5] Partial replacement of cobalt by aluminum leads to a decrease of B_c and to the appearance of weak itinerant ferromagnetism in Y(Al$_x$Co$_{1-x}$)$_2$ for $x > 0.12$.[6,7] In the case of magnetic RCo$_2$ compounds, long-range magnetic order of the 3d electron subsystem is induced by ordering of the localized magnetic moments of the rare earths. A substitution of Al on Co sites of the magnetic RCo$_2$ compounds, results in a considerable increase of the Curie temperature.[8]

This behavior was interpreted within the framework of the itinerant magnetism by an increase of the density of states (DOS) at the Fermi level as Co is replaced by Al. However, the mechanism, responsible for the increase of DOS at the Fermi level, remains obscure. Mainly two scenarios have been proposed: in the first, DOS increases due to depopulation of 3d-Co band when Co is replaced by Al[6,9]; in the second, the DOS increase is caused by a narrowing of the 3d band due to an expansion of the crystal lattice in the alloys.[7,10]

In the present work, we use the temperature-dependent thermopower $S(T)$ to study the mechanism of the DOS enhancement in Al-substituted RCo$_2$ compounds. It has been shown that $S(T)$ high-temperature minimum, observed in $S(T)$ of nearly all RCo$_2$ compounds in a range from 150 to 400 K, is associated with a sharp peak in the density of states related mainly to the Co 3d-electron density.[11] Particularly, it was shown that the temperature $T_{\min}$, at which the thermopower has this minimum, is a measure of the DOS peak width.[12,3]

Another unsolved problem, related to metamagnetism and charge transport in RCo$_2$ compounds is the different order of the phase transition at Curie temperature (T_C) and a nonmonotonic variation of the resistivity jump ($\Delta\rho$) at T_C. Among the RCo$_2$ compounds, ErCo$_2$, HoCo$_2$ and DyCo$_2$ undergo a first-order phase transition at T_C, whereas it is generally accepted that in TbCo$_2$, GdCo$_2$, TmCo$_2$, and SmCo$_2$, the magnetic ordering is via second-order transition. The kind of the phase transition at T_C in PrCo$_2$ and NdCo$_2$ has been a subject of recent discussion.[13–16] In this context, the Ho(Al$_x$Co$_{1-x}$)$_2$ alloys are proper materials to study, since this alloy system includes compounds with both, first-order and second-order transition at T_C.

I. EXPERIMENTAL PROCEDURES

The samples of Ho(Co$_{1-x}$Al$_x$)$_2$ alloys were prepared from pure components by melting in an induction furnace under a protective Ar atmosphere and were subsequently annealed in

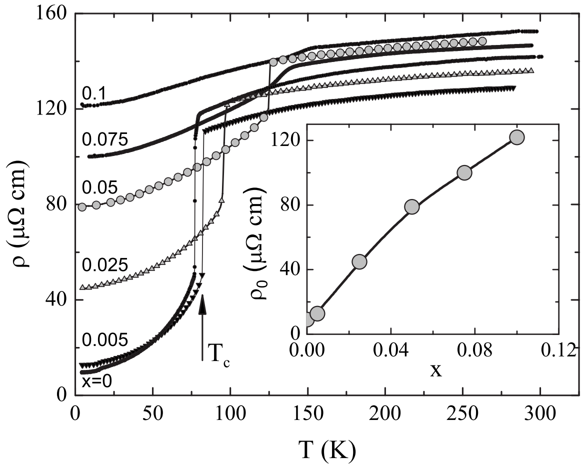

FIG. 1. Temperature dependent resistivity of $Ho(Co_{1-x}Al_x)_2$ for various Al concentrations. The inset shows the composition dependence of the residual resistivity, measured at 4.2 K.

vacuum at 1100 K for about one week. The x-ray analysis showed no traces of impurity phases.

A four-probe dc method was used for the electrical resistivity measurements; for the thermopower measurements, a differential method was applied. Typical size of the samples was about $1\times1\times10\ \text{mm}^3$. The estimated error in the absolute value of the electrical resistivity is $\pm10\%$. This is mainly due to uncertainty in the sample geometry which is closely related to the mechanical quality of the samples. The thermopower was measured with an accuracy of $\pm0.2\ \mu\text{V K}^{-1}$.

II. EXPERIMENTAL RESULTS

The resistivity temperature dependencies are depicted in Fig. 1. The residual resistivity, shown in the inset, rapidly increases with Al content. Simultaneously, the temperature-dependent part of the resistivity decreases, so that the high-temperature total resistivity shows a comparatively small change with composition. Room temperature values are in the range of 130 to 150 $\mu\Omega$ cm.

The Curie temperature is marked by an abrupt change of the resistivity of the samples with $x=0$, 0.005, 0.025, and 0.05, whereas samples with $x=0.075$ and 0.1 clearly show a second-order-like variation of the resistivity at T_C. Data of Fig. 1 indicate that the boundary between first-order and second-order transitions is between $x=0.05$ and $x=0.075$. These results agree with the data of Duc *et al.*[17]

Figure 2 presents experimental results for the thermopower from 5 to 300 K. Dramatic changes of $S(T)$ with the alloy composition are clearly seen in both, the paramagnetic and in the magnetically ordered state of the alloys. At high temperatures, the $S(T)$ minimum temperature $T_{\min}$, observable for pure $HoCo_2$ at 250 K, and the absolute $S(T)$ values decrease with increasing Al content. In the low-temperature region, $(T<T_C)$, $S(T)$ is also strongly dependent on the Al content.

At the lowest temperatures, all compounds exhibit a minimum with negative $S(T)$ values; its temperature gradually increases with Al concentration. The $S(T)$ minimum, as well at the following maximum, become suppressed for $x=0.05$ and they almost disappear for $x=0.075$. The Curie temperatures are associated with the discontinuous changes of $S(T)$ for $x=0$, 0.005, 0.025, whereas the sample with $x=0.075$ clearly shows a second-order-like variation of the thermopower at T_C.

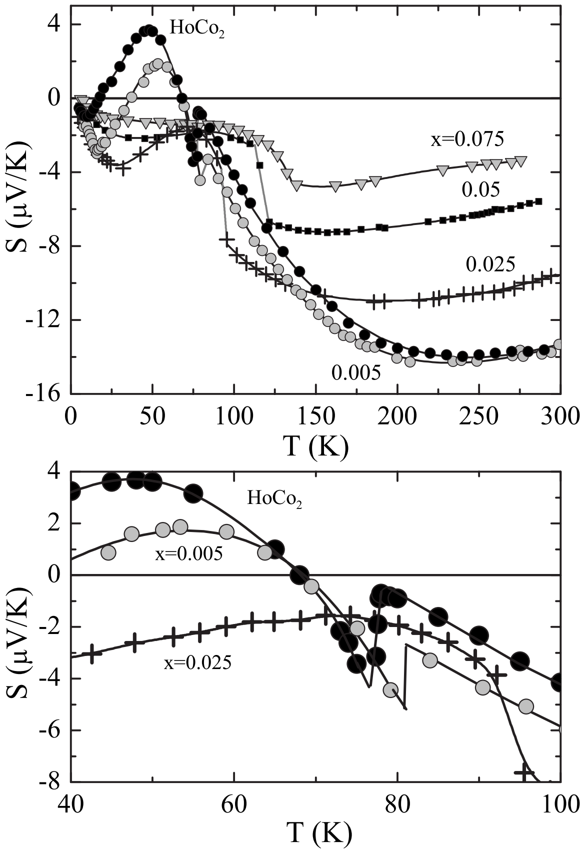

FIG. 2. Temperature dependent thermopower of $Ho(Co_{1-x}Al_x)_2$. The lower panel shows $S(T)$ of the $x=0$, $x=0.005$, and $x=0.025$ alloys in a vicinity of Curie temperature.

III. DISCUSSION

A. *Variation of the* 3*d*-DOS upon substitution of cobalt by nonmagnetic elements

The temperature variation of the thermopower in the paramagnetic temperature region can be understood within the model proposed in.[3,12,18] Calculations of the density of states, $N(\varepsilon)$ for YCo_2 [19–22] revealed the Fermi level, ε_F, lying near a sharp peak of DOS, primarily composed of 3*d* states of Co (Fig. 3).

Since Co is present in all RCo_2 compounds, it is assumed, that $N(\varepsilon)$ has the same general features throughout the RCo_2 series.

It has been shown that the high-temperature minimum, observed in $S(T)$ of nearly all RCo_2 compounds (with the exception of $GdCo_2$, $DyCo_2$, and $SmCo_2$ where $T_{\min}$ falls into the temperature range where these compounds order magnetically), is associated with the 3*d* peak of the DOS,

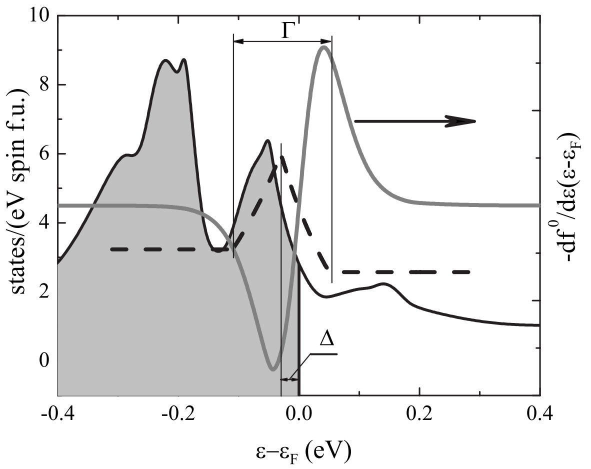

FIG. 3. DOS of RCo$_2$ compounds in a vicinity of the Fermi level (solid line) (Ref. 20). The gray line shows $-df^0/d\varepsilon(\varepsilon-\varepsilon_F)$ at $T=300$ K (f^0 is Fermi distribution function) to indicate the energy region important for transport properties. The broken line is the model state density, used for thermopower calculations. Γ is the width of the model DOS peak, Δ—is the distance from Fermi level to the center of the peak.

$T_{\min}$ being the measure of the peak width.[3,12]

Since the width of an itinerant electronic band depends on the extent of the corresponding atomic-orbital overlapping, one should expect that the $3d$ peak width increases when the lattice parameter decreases. The lattice parameter within RCo$_2$ compounds reveals considerable variation, being smallest for ScCo$_2$ and largest for NdCo$_2$. This implies that the $3d$ DOS peak width is largest in case of ScCo$_2$ and smallest for NdCo$_2$ with corresponding variation of $T_{\min}$. This assumption has been confirmed by a good correlation between $T_{\min}$ and the lattice constants of the RCo$_2$ compounds.[3] Figure 4(a) reproduces, in part, this correlation.

The decrease of $T_{\min}$ with increasing Al content in Ho(Co$_{1-x}$Al$_x$)$_2$ alloys [Fig. 4(b)] indicates a narrowing of the $3d$ DOS peak. Partially, this narrowing can be connected with the increase of the lattice parameter in the alloys. However, the expansion of the crystal lattice is insufficient to entirely account for the narrowing of the DOS peak and the observed increase of the Curie temperature. If the decrease of $T_{\min}$ was related only to the lattice expansion, then one would expect that $T_{\min}$ in the alloys decreases roughly at the same rate as in pure RCo$_2$ compounds. However, the results for Ho(Co$_{1-x}$Al$_x$)$_2$ reveal a much stronger dependence of $T_{\min}$ on the lattice parameter [Fig. 4(a)], implying that some additional factor is responsible for the narrowing of the peak width and increase of T_C.

Literature results on Y$_{1-t}$Lu$_t$(Co$_{1-x}$Al$_x$)$_2$ (Ref. 28) alloys with invariable lattice parameter show, that at small x (up to about $x=0.06-0.1$) the critical field for metamagnetic transition in these alloys decreases at the same rate as in Lu(Co$_{1-x}M_x$)$_2$ (M=Ga, Sn, Al) (Refs. 24 and 25) and Y(Co$_{1-x}$Al$_x$)$_2$ (Refs. 26 and 27) alloys, where lattice parameter varies considerably. Similarly, in Ho(Co$_{1-x}$Si$_x$)$_2$ diluted alloys[23] with invariable lattice parameter and in Ho(Co$_{1-x}$Al$_x$)$_2$ alloys T_C increases with x at the same rate, see Fig. 4(b). This indicates, in agreement with our results, that lattice expansion cannot be the main cause for the magnetic enhancement of the alloys. On the other hand, the $3d$ band depopulation model also cannot explain these results since the substituting elements have different configurations of the outer electronic shells.

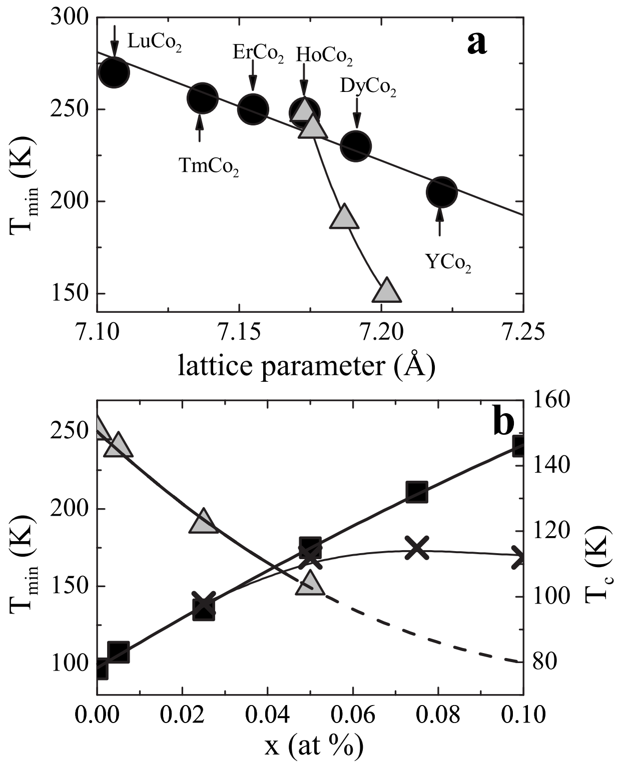

FIG. 4. (a) Dependence of $T_{\min}$ against lattice parameter for RCo$_2$ compounds (●—data from Ref. 3). The triangles show this work results for Ho(Co$_{1-x}$Al$_x$)$_2$ alloys. (b) $T_{\min}$ (triangles) and Curie temperature T_C (■) against composition for Ho(Co$_{1-x}$Al$_x$)$_2$. ×—T_C against composition for Ho(Co$_{1-x}$Si$_x$)$_2$ alloys according to Ref. 23.

The results show that the mechanism, which causes the decrease of B_c in nonmagnetic compounds (or increase of T_C in the magnetic ones) does depend at small x neither on the type of substituting element nor on the lattice expansion. What all above mentioned alloys have in common is the disorder within the Co sublattice due the substitution of Co by other elements. We therefore conclude that the principal reason for the narrowing of the $3d$ band in Ho(Co$_{1-x}$Al$_x$)$_2$ for low Al contents is the increasing localization of the $3d$ electrons caused by disorder within Co sublattice. Experimental results on transport in Y(Co$_{1-x}$Al$_x$)$_2$ alloys has led us to a similar conclusion.[29] A different situation takes place when the impurity element has unfilled $3d$-shell, such as Ni and Fe, in that case the effects of the change of $3d$ electron concentration play a dominant role.[30]

Of course, one cannot exclude a change of the $3d$ electron concentration upon the Co substitution in Ho(Co$_{1-x}$Al$_x$)$_2$. Moreover, the decrease of $S(T)$ values in the paramagnetic temperature region, as will be demonstrated later, implies such a change. It also follows from literature that the behavior of Y(Co$_{1-x}M_x$)$_2$ alloys at large x (above about 0.1), such as the stabilization of a ferromagnetic ground state, depends on the kind of substituting elements, suggesting a hybridiza-

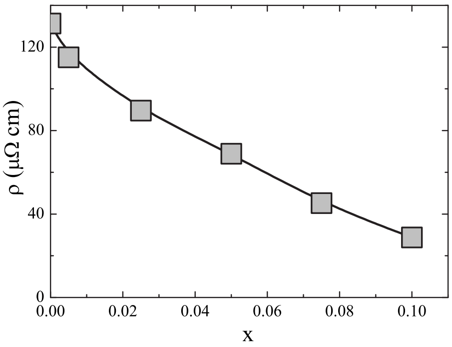

FIG. 5. Temperature-induced part of resistivity $\rho(250)-\rho(4.2)$ of $Ho(Co_{1-x}Al_x)_2$ alloys.

tion of *s*-*p* and 3*d* states. However, our analysis shows that the change of the 3*d* electron concentration does not play major role in magnetic enhancement of diluted alloys.

To summarize this part, our experimental results on transport properties of $Ho(Co_{1-x}Al_x)_2$ alloys and analysis of the results, reported in the literature, led us to the conclusion that the principal mechanism, responsible for the increase of T_c in magnetic alloys, or a decrease of B_c in paramagnetic alloys, is the narrowing of the 3*d* DOS peak due to localization of Co 3*d* electron states, induced by disorder in Co sublattice of the alloys.

B. Electrical resistivity

The rapid increase of the residual resistivity and the modest variation of high-temperature resistivity with Al content are the most important characteristic features observed in the resistivity of the alloys. The temperature-dependent part of the resistivity systematically decreases with *x* as it is shown in Fig. 5. We should note that such behavior is common for many RCo_2-based alloys,[23,26,31–35] which include both, $R(Co_{1-x}M_x)_2$ and $Y_{1-x}R_xCo_2$ systems.

However, there has been no commonly accepted model able to account for the observed variation of the temperature-dependent resistivity. The independence of the phenomenon on the constituents of the alloys implies a common mechanism. As in the case of the above discussed Co localization, disorder and metamagnetism of the magnetic Co subsystem are the natural candidates. Baranov *et al.*[36,37] were probably the first to emphasize the important role which disorder can play in RCo_2-based alloys. In a certain range of alloy composition, 3*d* magnetic subsystem can be in "partially" ordered ground state, i.e., in the alloy there are spatial regions with high and low 3*d* magnetization. This static magnetic disorder originates from a combination of fluctuating exchange field (in $(Y_{1-x}R_x)Co_2$ alloys), or fluctuating local susceptibility (in $R(Co_{1-x}M_x)_2$ alloys), and of the metamagnetism of 3*d* electron system. Scattering of conduction electrons of this static magnetic disorder gives contribution to the alloy resistivity, which is comparable to the high-temperature limit of 3*d* spin-fluctuation (SF) resistivity (the resistivity due to scattering on dynamic, i.e., temperature-induced, fluctuations of local 3*d* magnetization) in RCo_2 compounds.[38] The static magnetic disorder can be viewed as "frozen" SF. When temperature increases, this frozen disorder melts and is replaced by the dynamic disorder. Since the corresponding contributions to resistivity are of similar magnitude, the temperature variation of the total resistivity is considerably reduced.

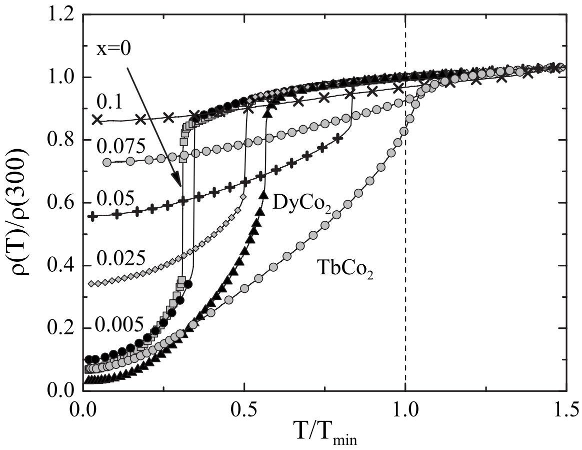

FIG. 6. Normalized resistivity $\rho(T)/\rho(300)$ against normalized temperature $T/T_{\min}$ for $Ho(Co_{1-x}Al_x)_2$ alloys and $DyCo_2$, $TbCo_2$ compounds. (Ref. 39)

Figure 6 shows the resistivity of $Ho(Co_{1-x}Al_x)_2$, $DyCo_2$ and $TbCo_2$,[39] normalized to its value at $T=300$ K, plotted against $T/T_{\min}$ to account for the different width of the 3*d* band. Since for the $Ho(Co_{1-x}Al_x)_2$ with $x>0.075$ the high-temperature minimum in $S(T)$ is not observable due to the high T_C, we use an interpolation of $T_{\min}(x)$, as it is shown in Fig. 4(b) by the broken line, to obtain $T_{\min}$ of these alloys.

The other two interesting features of the resistivity can be seen from Fig. 6:

(1) The kind of the phase transition at Curie point is changed from first to second order around $T_C=T_{\min}$. This is another manifestation that $T_{\min}$ is an essential physical parameter, directly reflecting DOS features. The relation between $T_{\min}$ and the change of the transition order follows from the model of the metamagnetic transition of Co subsystem[2] as a consequence of the temperature smearing of DOS features at the Fermi level.[2,17]

Essentially, the same mechanism leads to the development of the minima in $S(T)$.[12] There is, however, an alternative theoretical model in which the order of a magnetic phase transition depends basically on the lattice-constant value.[40] Since the width of the DOS peak (and, therefore, $T_{\min}$) is determined in pure RCo_2 compounds by the lattice parameter, $T_C/T_{\min}\approx 1$ represents a more general condition for the boundary between second- and first-order phase transition in these compounds.

(2) The magnitude of the resistivity drop at the Curie temperature $\Delta\rho(T_C)$ decreases as T_C approaches $T_{\min}$. This last feature is also present in binary RCo_2 compounds, as it can be seen comparing the resistivities of $HoCo_2$ and $DyCo_2$, shown in Fig. 6. The resistivity drop at T_C of heavy RCo_2 compounds, which exhibit a first-order transition, has been attributed to a sudden suppression of SF by strong molecular field of the ordered 4*f* moments.[3] This, however, does not explain the decrease of $\Delta\rho(T_C)$ with increasing T_c. We pro-

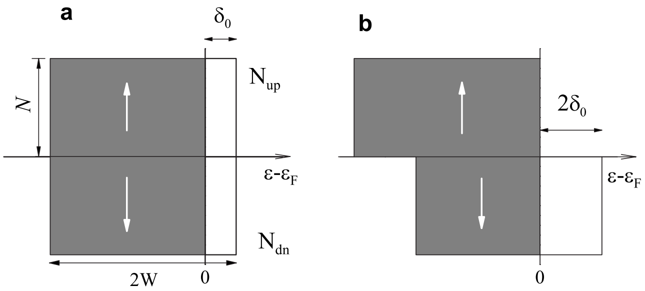

FIG. 7. The model of $3d$ DOS: (a) Nonpolarized state at $T=0$ K; (b) Polarized state at $T=0$ K. $2W$ is the $3d$ band width, δ_0 is the distance from Fermi energy to the top of $3d$ band and N-DOS magnitude.

pose that the origin of this decrease is the same as the origin of resistivity saturation of nearly magnetic compounds at high temperatures.[41,42] In the model, put forth in[41,42] by Ueda and Moriya, the SF contribution to the resistivity (ρ_{sf}) is determined by the d band dynamical susceptibility, which is enhanced due to d band SF. It has been shown that the saturation tendency, which is characteristic for the temperature-dependent resistivity of nearly magnetic materials, originates from the strong decrease of the d band enhancement owing to interactions among SF at high temperatures.

We use here a very simplified model with a rectangular approximation for the Co $3d$ DOS (Fig. 7) to illustrate the essential physics of the resistivity saturation and of the decrease of $\Delta\rho(T_C)$.

We consider an enhanced $3d$ band paramagnetic compound (such as $\mathrm{YCo_2}$). At $T=0$ K, without external field, the spin-up and spin-down subbands are equally occupied, Fig. 7(a), and there are no SF. At a nonzero temperature, thermal fluctuations of the $3d$ subband occupation, amplified by exchange interaction, result in fluctuations of local magnetization, i.e., SF. According to Ref. 42, the magnitude of the local magnetization fluctuations $(\langle m^2\rangle)^{1/2}$ increases with temperature, however, it saturates at a constant value in a high-temperature limit. Both the saturation value and crossover temperature are determined by the $3d$ band parameters.

In magnetic $R\mathrm{Co_2}$ compounds, the $3d$ system at $T=0$ K is in high magnetization state. In the following, we consider $3d$ band in this case as fully polarized by the exchange field of ordered $4f$ moments, as schematically shown in Fig. 7(b), with saturation magnetic moment $M_f=2N\delta_0$. As temperature increases, there will also be temperature-induced fluctuations of the $3d$ magnetization around this polarized state.

For our qualitative model, we assume that the SF resistivity is determined by the spin-spin correlation function

$$\langle m(0)m(l)\rangle - \langle m(0)\rangle\langle m(l)\rangle ,$$

where $m(0)$ and $m(l)$ are the local $3d$ magnetization at lattice point with coordinates $r=0$ and $r=l$, respectively, and l is distance of order of conduction-electron (s-electron) mean-free path. The scattering magnitude of conduction electron by a magnetic fluctuation is proportional to its squared magnitude, measured relative to the local background at a distance of order of conduction-electron mean-free path. Therefore, the most effective will be the scattering on correlated magnetic fluctuations with largest difference of local magnetization at points $r=0$ and $r=l$. For the paramagnetic state, this corresponds to fluctuations at $r=0$ and $r=l$ with the opposite magnetization. While for a system in ferromagnetic ground state with fully polarized $3d$ band, the largest difference is between this fully polarized state moment M_{f} and local fluctuation with a reduced moment. Basing on the above arguments, we define the effective SF magnitude (m_{p}-paramagnetic state, m_{f}-ferromagnetic state), determining the SF resistivity as

$$m_p \propto 2(D_{\mathrm{up}} - D_{\mathrm{dn}}), \qquad (1)$$

where

$$D_{\mathrm{up(dn)}} = \int_{-(2W-\delta_0 \pm (\mp)\zeta k_B T)}^{\infty} N f^0 d\varepsilon ,$$

and

$$m_f \propto M_f - (D_{\mathrm{up}} - D_{\mathrm{dn}}), \qquad (2)$$

with

$$D_{\mathrm{up}} = \int_{-(2W-\zeta k_B T)}^{\infty} N f^0 d\varepsilon$$

and

$$D_{\mathrm{dn}} = \int_{-(2W-2\delta_0+\zeta k_B T)}^{\infty} N f^0 d\varepsilon .$$

The definitions of W, δ_0, and N are given in Fig. 7. D_{up} and D_{dn} are local spin-up and spin-down density, f^0 is the Fermi distribution function, and ζ is the exchange enhancement factor.

Due to the charge neutrality condition ($D_{\mathrm{up}}+D_{\mathrm{dn}}=\mathrm{const}$), the magnitude of the SF has an upper limit. Both m_p and m_f have maximum value of $4N\delta_0$. For the unpolarized $3d$ band, the SF attain the maximum amplitude at a temperature T_m satisfying condition $\zeta k_B T_m = \delta_0$, whereas for the fully polarized $3d$ band, the corresponding condition is $\zeta k_B T_m = 2\delta_0$. At higher temperatures, the itinerant SF behaves as localized magnetic moments with fixed magnitude.

The corresponding SF resistivity follows from Eqs. (1) and (2):

$$\rho_p \propto (m_p)^2 \propto \begin{cases} (4N\zeta k_B T)^2 & \text{if } T \le \dfrac{\delta_0}{\zeta k_B} \\ (4N\delta_0)^2 & \text{if } T > \dfrac{\delta_0}{\zeta k_B} \end{cases} ,$$

for the nonpolarized (paramagnetic) state, and

$$\rho_f \propto (m_f)^2 \propto \begin{cases} (2N\zeta k_B T)^2 & \text{if } T \le \dfrac{2\delta_0}{\zeta k_B} \\ (4N\delta_0)^2 & \text{if } T > \dfrac{2\delta_0}{\zeta k_B} \end{cases} ,$$

for the polarized (magnetically ordered) $3d$ band. Expression for ρ_p gives a roughly correct representation of the overall temperature dependence of the SF resistivity of paramagnetic

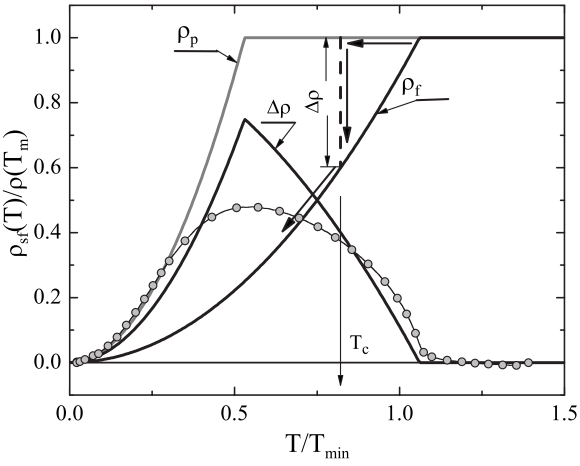

FIG. 8. Schematic temperature dependence of normalized ρ_{sf} for polarized (ρ_f) and nonpolarized (ρ_p) states of the $3d$ band and temperature dependence of resistivity jump at first-order transition from nonpolarized to polarized (ferromagnetic) state $\Delta\rho=\rho_p-\rho_f$. The circles show the experimental difference between the normalized resistivities of paramagnetic YCo_2 and ferrimagnetic $TbCo_2$ (Ref. 39). The temperature is normalized to T_{min} of $TbCo_2=214$ K (Ref. 3). $T_m=\frac{2\delta_0}{\zeta k_B}$.

RCo_2 compounds: it increases as T^2 at low temperatures and saturates to a temperature-independent value at high temperatures.[3]

Both, ρ_p and ρ_f are displayed in Fig. 8.

In RCo_2 compounds with a first-order magnetic phase transition, the $3d$ band undergoes at T_C a transition from the nonpolarized to the polarized state (shown schematically by the arrows in Fig. 8), with corresponding change of the SF resistivity: $\Delta\rho=\rho_p-\rho_f$, which is also presented in Fig. 8. For comparison, the experimental difference between the normalized resistivity of paramagnetic YCo_2 (Ref. 39) (a representative of a nonpolarized state of the $3d$ band) and of ferrimagnetic $TbCo_2$ (Ref. 39) (a representative of the polarized state of the $3d$ band) is shown on this figure too. In spite of very schematic model, used to calculate $\Delta\rho$, there is close correspondence between theoretical and experimental curve.

The experimental resistivity jump observed at T_C of RCo_2 and $Ho(Co_{1-x}Al_x)_2$ is presented in Fig. 9. $\Delta\rho(T_C)$ is shown for pure $TmCo_2$,[44] $ErCo_2$, $HoCo_2$, and $DyCo_2$ (Ref. 39) compounds and for $Ho(Co_{1-x}Al_x)_2$ alloys. Also shown are the results for $ErCo_2$, $HoCo_2$, and $DyCo_2$ under pressure up to 16 kbar.[43] The resistivity drop is plotted against T_C/T_{min} to account for the different width of Co-$3d$ band.

We do not have experimental data on thermopower of all RCo_2 under pressure, therefore the same value of $\frac{dT_{\text{min}}}{dP}=0.7$ K/kbar was used to calculate T_{min} for compounds under pressure, shown in Fig. 9. $\frac{dT_{\text{min}}}{dP}$ was obtained experimentally for a $(Gd_{0.01}Y_{0.99})Co_2$ alloy.[45] As it can be seen from Fig. 9, there is qualitative agreement between theoretical and experimental values of $\Delta\rho$. The model shows two important features in the resistivity behavior: the saturation at high temperatures, and the decrease of $\Delta\rho(T_C)$ with increasing T_C. The important parameters of the model are the bandwidth $2W$ and the distance from the Fermi level to band edge δ_0. They can be estimated in the following way. The empty portion of the $3d$ band can be evaluated from the experimentally observed saturation Co-moment $M=1$ μ_B/Co for RCo_2 compounds. From this value it follows that $\delta_0\approx0.1W$. Using the experimentally observed temperature range in which $\Delta\rho$ is nonzero (Fig. 9) as the measure for δ_0 (200 K), and taking $\zeta=7$ (Ref. 22) (which gives $\delta_0\approx0.12$ eV), we get for Co-$3d$ bandwidth $2W$ about 2.4 eV, in a very reasonable agreement with the value of 2.5 eV, according to the result of Ref. 22.

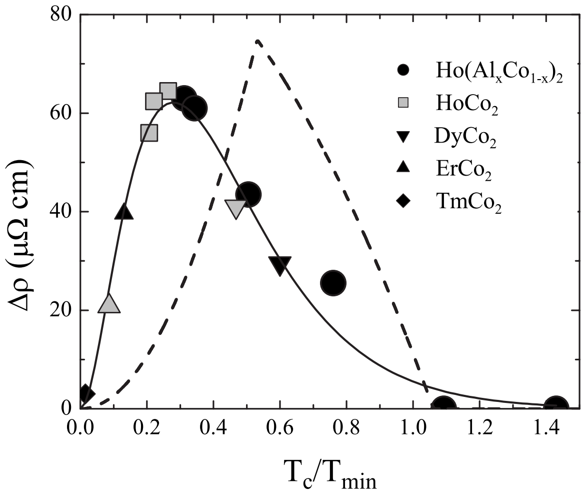

FIG. 9. The resistivity drop $\Delta\rho$ at Curie temperature of $Ho(Co_{1-x}Al_x)_2$ alloys and of some RCo_2 compounds (Refs. 39 and 44) Broken line is theoretical $\Delta\rho$, scaled with $\rho(T_m)=100$ $\mu\Omega$ cm. The gray symbols stand for data under pressure for corresponding compounds (Ref. 43).

The model DOS used here to demonstrate the mechanism of $\Delta\rho(T_C)$ decrease with increasing T_C, is obviously too oversimplified to account for the very details of $\rho_{\text{sf}}(T)$ and $\Delta\rho(T_C)$. The omission of $4f$-$3d$ exchange interaction is less obvious. This effect, however, is clearly visible, if one compares $\rho(T)$ of paramagnetic and magnetic RCo_2 compounds, depicted in Fig. 10.

For a hypothetical magnetic RCo_2 compound, whose resistivity includes only SF, phonon, and impurity contributions, its normalized resistivity above T_C would coincide with the normalized resistivity of paramagnetic YCo_2, while below T_C, it should be similar to the normalized resistivity of $TbCo_2$. However, as we can see from Fig. 10, the normalized resistivity of the other magnetic RCo_2 compounds deviates on approach to T_C from the resistivity of $TbCo_2$ at $T<T_C$ and from the resistivity of YCo_2 at $T>T_C$. In part, this deviation refers to additional contributions owing to scattering on $4f$ magnetic moments in magnetic RCo_2. At $T>T_C$, the corresponding contribution, ρ_{spd}, is independent of temperature. Therefore, the normalized resistivity of a magnetic compound:

$$\frac{\rho(T)}{\rho(300)}=\frac{\rho_{YCo_2}(T)+\rho_{\text{spd}}}{\rho_{YCo_2}(300)+\rho_{\text{spd}}}$$

differs from the normalized resistivity of YCo_2.

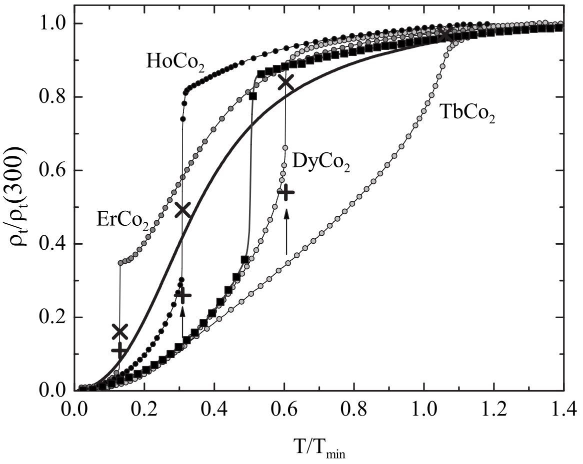

FIG. 10. Normalized resistivity of RCo$_2$ compounds (Ref. 39) and Ho(Co$_{0.975}$Al$_{0.025}$)$_2$ alloy (■). The solid line is the resistivity of YCo$_2$, $\rho_t=\rho(T)-\rho(4.2)$, ×, and + indicate resistivity at T_C, including corrections for ρ_{spd} and ρ_{sw} in paramagnetic and ferrimagnetic phase, respectively.

Below T_C, instead of ρ_{spd} there is a temperature-dependent 4f spin-wave contribution to the resistivity, ρ_{sw}. It increases with temperature, reaching at T_C a maximum value. In ferromagnetic metals with second-order phase transition, $\rho_{sw}(T_C)\approxeq\rho_{spd}$; however, in RCo$_2$ with first-order transition, it should be strongly suppressed by the 3d exchange field just below the transition. The estimated resistivity at T_C, including contributions of ρ_{spd} or ρ_{sw}, is shown in Fig. 10. For these estimations we use $\rho_{sw}(T_C)=\rho_{spd}$, with ρ_{spd} from Ref. 3. Corrections due to ρ_{sw} are certainly overestimated. Nevertheless, it is clear from Fig. 10 that these corrections cannot account for the observed deviations, especially above T_C. The origin of these deviations is the mutual interaction between the 4f and the 3d magnetic systems. Below T_C, the spin-wave excitations in the 4f system amplify the itinerant SF of the 3d polarized band, leading to strong increase of the resistivity on approaching T_C. In the paramagnetic state there is a similar mutual amplification of 4f and 3d SF on approach to T_C from higher temperatures. This amplification increases with decreasing T_C since the susceptibility of the localized 4f moments increases with decreasing temperature.

C. Thermopower

$S(T)$ above T_C is related to DOS features in vicinity of the Fermi energy. Results for Ho(Co$_{1-x}$Al$_x$)$_2$ alloys provide further support to the model outlined in our previous publications.[12,18]

We use similar approach and the model DOS, depicted in Fig. 3 by the dotted line, to explore the dependence of the thermopower on Co 3d band parameters. According to Mott's s-d model, the conductivity is due to high mobility s-electron states, from which the charge carriers are scattered into 3d states with low mobility and, effectively, are eliminated from conduction process. The scattering probability of conduction electrons is proportional to the state-density value, into which an electron is scattered. Therefore, within s-d model, the s–electron-scattering probability P is expected to depend on the electron energy as:

$$P(\varepsilon-\varepsilon_F)\propto N_d(\varepsilon-\varepsilon_F)+R, \tag{3}$$

where R is due to other than s-d scattering transitions. This relation is valid for elastic or quasielastic scattering.

Thermopower is expressed as[18,46]

$$S(T)=-\frac{1}{|e|T}\frac{\int_0^\infty \omega(\varepsilon,T)\left(-\frac{\partial f^0}{\partial\varepsilon}\right)(\varepsilon-\varepsilon_F)d\varepsilon}{\sigma(T)}, \tag{4}$$

where

$$\sigma(T)=\int_0^\infty \omega(\varepsilon,T)\left(-\frac{\partial f^0}{\partial\varepsilon}\right)d\varepsilon \tag{5}$$

and

$$\omega(\varepsilon,T)=\frac{e^2}{12\pi^3\hbar}vA(\varepsilon)\tau(\varepsilon,T), \tag{6}$$

where v is the velocity of conduction electrons, $A(\varepsilon)$ is the cross-sectional area of the Fermi surface perpendicular to the electrical field direction. $\tau\propto\frac{1}{P}$ is the relaxation time. In the s-d model approximation,

$$\tau(\varepsilon-\varepsilon_F)\propto\frac{1}{N_d(\varepsilon-\varepsilon_F)+R}. \tag{7}$$

Using Eqs. (4)–(7), $S(T)$ is calculated with the model DOS, shown in Fig. 3. The results of the calculations are shown in Fig. 11. The calculations were performed using different values of two parameters describing the model DOS: Γ is the width of the 3d DOS peak, and Δ—is the distance from Fermi energy to the center of the peak.

Two important conclusions follow from these results:

(1) The position of the thermopower minimum depends mainly on the 3d peak width;

(2) The depopulation of the 3d band affects the magnitude of the high-temperature thermopower, however, it has almost no effect on the position of the thermopower minimum.

Comparison of the theoretical result of Fig. 11(c) and experimental data on thermopower (Fig. 2) indicates that both effects—depopulation and narrowing of 3d band, play an important role determining $S(T)$ in the paramagnetic temperature range. Both also lead to an increase of 3d DOS at Fermi level. From the variation of parameters Δ and Γ, we can roughly estimate that the narrowing of 3d band increases DOS at Fermi level by more than 50%, while depopulation—by less than 20%. Therefore, this estimation support our conjecture, that narrowing of 3d band due to disorder plays dominant role in the magnetic enhancement of R(Co$_{1-x}M_x$)$_2$ alloys.

The calculations of thermopower were made under assumption of elastic scattering, which is valid at high temperatures, i.e., above about 100 K. At lower temperatures scattering on SF is nonelastic. The distinction between elastic and nonelastic scattering is essential in case of thermopower (however, it is not important for resistivity). For elastic scattering, the change of conduction-electron energy

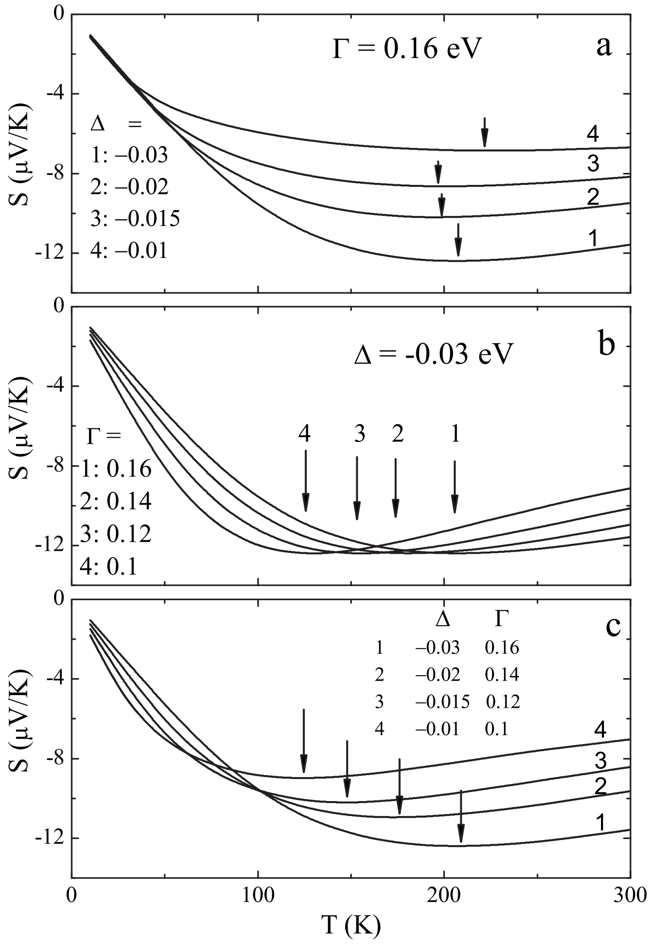

FIG. 11. The temperature dependencies of thermopower calculated within *s*-*d* scattering model approximation. (a) The DOS peak width is fixed at $\Gamma = 0.16$ eV, the distance from the Fermi energy to the center of the DOS peak, Δ, varies, simulating the depopulation of the 3*d* band. (b) The occupation of the 3*d* band Δ is fixed at −0.03 eV, the width of the 3*d* peak varies. (c) Both, Γ and the absolute value of Δ decrease. The arrows indicate position of the thermopower minimum.

satisfies the condition: $|\varepsilon(k') - \varepsilon(k)| \ll k_B T$, where k' and k denote the final and initial states, respectively. In nonelastic scattering, the change of the electron energy in a scattering event is of order of $k_B T$. On average, an electron from a state above ε_F will be scattered into a state below ε_F and vice versa. Therefore, while for elastic scattering (due to negative $\frac{dN_d}{d\varepsilon}$ values at Fermi energy) $\tau(\varepsilon > \varepsilon_F) > \tau(\varepsilon < \varepsilon_F)$, for the nonelastic scattering it can be reversed: $\tau(\varepsilon > \varepsilon_F) < \tau(\varepsilon < \varepsilon_F)$, leading to a positive thermopower instead of negative values for elastic scattering. The effect of these different scattering regimes is clearly visible in $S(T)$ of paramagnetic $R\text{Co}_2$ compounds:[3] with decreasing temperature below about 100 K, $S(T)$ shows a clear tendency to change sign, which, however, is interrupted by another process, leading to large negative thermopower values at low temperatures. This process is likely caused by SF drag effect.

$S(T)$ of $\text{Ho}(\text{Co}_{1-x}\text{Al}_x)_2$ at $T < T_C$ exhibits a complicated variation as obvious from Fig. 12.

Data imply that these temperature dependencies result from an interplay between impurity (elastic) and spin-wave (nonelastic) scattering. For diluted alloys at low temperatures, the impurity scattering constitutes the main contribution to thermopower. This gives rise to negative $S(T)$ values, exhibiting an almost linear temperature variation. At higher temperatures, nonelastic scattering on spin waves becomes important and results in the pronounced positive peak, especially at lower Al content. According to the Nordheim-Gorter rule,[46] thermopower of a conductor with two dominating scattering processes, can be expressed as:

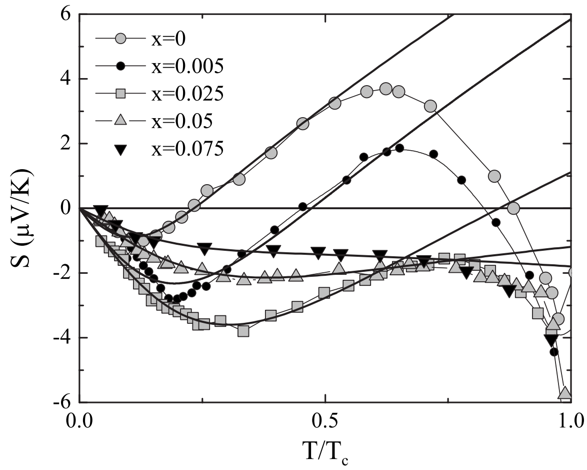

FIG. 12. Low temperature thermopower of $\text{Ho}(\text{Co}_{1-x}\text{Al}_x)_2$. The solid lines represent the Nordheim-Gorter expression (9) with parameters listed in Table I.

$$S = \frac{S_0 \rho_0}{\rho} + \frac{S_{sw} \rho_{sw}}{\rho}, \tag{8}$$

with $\rho = \rho_0 + \rho_{sw}$. The subscripts refer to impurity and spin-wave scattering contributions. The resistivity related to scattering on spin waves follows from $\rho_{sw} = AT^2$. We assume that both, S_0 and S_{sw}, are linear at low temperatures: $S_0 = b_0 T$, and $S_{sw} = b_{sw} T$. Based on these assumptions, we obtain for the total thermopower:

$$S = \frac{T}{1 + \left(\frac{T}{T_0}\right)^2} \left[b_0 + b_{sw} \left(\frac{T}{T_0} \right)^2 \right], \tag{9}$$

where T_0 is temperature, defined from the condition:

$$AT_0^2 = \rho_0.$$

Expression (9) was fitted to the low-temperature experimental thermopower using b_0, b_{sw}, and T_0 as free parameters. The results are shown in Fig. 12 by solid lines, and the parameter values are listed in Table I. For diluted alloys ($x = 0$, $x = 0.005$), the parameters are reasonable and show expected dependencies on x: b_0 and T_0 increase with x, while b_{sw} is independent of x. At larger values of x, however, the dominant low-temperature scattering mechanism is due to static magnetic disorder, related to the formation of a partially-ordered ground state of the 3*d* electron system. This scattering is not temperature independent, which leads to a decrease of b_0 and b_{sw} in concentrated alloys.

TABLE I. Fitted parameters of Eq. (8)

x	b_0	b_{sw}	T_0
0	−0.18	0.12	15
0.005	−0.25	0.1	24
0.025	−0.22	0.05	39
0.05	−0.09	0.0037	49
0.075	−0.055	−0.001	40

IV. CONCLUSION

In conclusion, we have studied electrical resistivity and thermoelectric power of $\mathrm{Ho(Co_{1-x}Al_x)_2}$ alloys ($0 \leq x \leq 0.1$) for temperatures from 4.2 to 300 K. The experimental temperature dependencies of thermopower indicate that the width of the Co 3*d* band decreases with Al content. This decrease cannot be accounted for only by the increasing lattice parameter of the alloys. The analysis of experimental results on magnetic and transport properties of $\mathrm{Ho(Co_{1-x}Al_x)_2}$ and other $R\mathrm{(Co_{1-x}}M_x\mathrm{)_2}$ alloys led us to the conclusion that the principal mechanism responsible for the narrowing of the 3*d* DOS peak is the localization of the Co 3*d* electron states, induced by disorder in Co sublattice of the alloys. The narrowing of the 3*d* DOS gives main contribution to enhancement of DOS at Fermi energy and to increase of T_C in magnetic alloys, or a decrease of B_c in paramagnetic alloys. This new mechanism of a magnetic enhancement of the Co 3*d* band in $R\mathrm{Co_2}$-based alloys upon substitution of Co by nonmagnetic elements reconciles two previous, apparently conflicting, models.

The magnitude of the resistivity jump at Curie temperature, observable in $\mathrm{Ho(Co_{1-x}Al_x)_2}$ and $R\mathrm{Co_2}$ compounds, exhibiting first-order magnetic phase transition, is a nonmonotonic function of T_C. Our simple model shows that the nonmonotonous variation of the resistivity jump with T_C is due to the saturation of the 3*d* band SF magnitude at high temperatures.

We postulate that fluctuations of the local magnetic susceptibility in $\mathrm{Ho(Co_{1-x}Al_x)_2}$ leads to development of partially-ordered ground state of the 3*d* magnetic subsystem, as it was shown previously for $\mathrm{Y}_{1-x}R_x\mathrm{Co_2}$ alloys (R are magnetic rare-earth elements). Static magnetic disorder, associated with this partially-ordered ground state, induces the huge residual resistivities observed. With increasing temperature, the static magnetic disorder is replaced by dynamic, temperature-induced SF. The corresponding contributions to the resistivity have similar magnitude. Therefore, the overall temperature variation of the resistivity in the alloys is strongly suppressed.

Our analysis demonstrate that the temperature behavior of the thermopower above 100 K is determined by a narrow peak in the 3*d* DOS at the Fermi energy. The complex behavior of the thermopower at low temperatures results from an interplay of elastic impurity scattering and nonelastic temperature-induced SF scattering.

ACKNOWLEDGMENTS

We want to thank A. Yu. Zyuzin for stimulating discussions. This work was supported by Russian Foundation for Basic Research under Grants No. 05-02-17816-a and No. 06-02-17047-a.

---

[1] R. Lemaire, Cobalt (Engl. Ed.) **32**, 132 (1966); **33**, 201 (1966).

[2] R. Z. Levitin and A. S. Markosyan, Sov. Phys. Usp. **31**, 730 (1988).

[3] E. Gratz, R. Resel, A. T. Burkov, E. Bauer, A. S. Markosyan, and A. Galatanu, J. Phys.: Condens. Matter **7**, 6687 (1995).

[4] T. Goto, K. Fukamishi, T. Sakakibara, and H. Komatsu, Solid State Commun. **72**, 945 (1989).

[5] T. Goto, T. Sakakibara, K. Murata, K. Komatsu, and K. Fukamichi, J. Magn. Magn. Mater. **90/91**, 700 (1990).

[6] V. V. Aleksandryan, A. S. Lagutin, R. Z. Levitin, A. S. Markosyan, and V. V. Snegirev, Sov. Phys. JETP **62**, 153 (1985).

[7] K. Yoshimura and Y. Nakamura, Solid State Commun. **56**, 767 (1985).

[8] V. V. Aleksandryan, K. P. Belov, R. Z. Levitin, A. S. Markosyan, and V. V. Snegirev, JETP Lett. **40**, 815 (1984).

[9] R. Ballou, Z. M. Gamishidze, R. Lemaire, R. Z. Levitin, A. S. Markosyan, and V. V. Snegirev, Sov. Phys. JETP **75**, 1041 (1993).

[10] K. Ishiyama and K. Endo, J. Phys. Soc. Jpn. **55**, 2535 (1986).

[11] This DOS feature is responsible for the itinerant metamagnetism of $R\mathrm{Co_2}$ compounds.

[12] A. T. Burkov, M. V. Vedernikov, and E. Gratz, Solid State Commun. **67**, 1109 (1988).

[13] M. Forker, S. Müller, P. de la Presa, and A. F. Pasquevich, Phys. Rev. B **68**, 014409 (2003).

[14] M. Forker, S. Müller, P. de la Presa, and A. F. Pasquevich, Phys. Rev. B **75**, 187401 (2007).

[15] J. Herrero-Albillos, F. Bartolomè, L. M. García, F. Casanova, A. Labarta, and X. Batlle, Phys. Rev. B **73**, 134410 (2006).

[16] J. Herrero-Albillos, F. Bartolomè, L. M. García, F. Casanova, A. Labarta, and X. Batlle, Phys. Rev. B **75**, 187402 (2007).

[17] N. H. Duc, T. D. Hien, R. Z. Levitin, A. S. Markosyan, P. E. Brommer, and J. J. M. Franse, Physica B (Amsterdam) **176**, 232 (1992).

[18] A. T. Burkov, E. Gratz, E. Bauer, and R. Resel, J. Alloys Compd. **198**, 117 (1993).

[19] M. Cyrot and M. Lavagna, J. Phys. (Paris) **40**, 763 (1979).

[20] H. Yamada, J. Inoue, K. Terao, S. Kanda, and M. Shimizu, J. Phys. F: Met. Phys. **14**, 1943 (1984).

[21] H. Yamada, Physica B (Amsterdam) **149**, 390 (1988).

[22] S. Tanaka and H. Harima, J. Phys. Soc. Jpn. **67**, 2594 (1998).

[23] N. H. Duc and T. K. Oanh, J. Phys.: Condens. Matter **9**, 1585 (1997).

[24] K. Murata, K. Fukamichi, H. Komatsu, T. Sakakibara, and T. Goto, J. Phys.: Condens. Matter **3**, 2515 (1991).

[25] K. Murata, K. Fukamichi, T. Sakakibara, T. Goto, and K. Suzuki, J. Phys.: Condens. Matter **5**, 1525 (1993).

[26] D. Michels, J. Timlin, and T. Mihhlisin, J. Appl. Phys. **67**, 5289

(1990).

[27] H. Wada, M. Hada, K. N. Ishihara, M. Shiga, and Y. Nakamura, J. Phys. Soc. Jpn. **59**, 2956 (1990).

[28] I. L. Gabelko, R. Z. Levitin, A. S. Markosyan, V. I. Silantiev, and V. V. Snegirev, J. Magn. Magn. Mater. **94**, 287 (1991).

[29] T. Nakama, K. Shintani, M. Hedo, H. Niki, A. T. Burkov, and K. Yagasaki, Physica B **281&282**, 699 (2000).

[30] T. Goto, H. Aruga Katori, T. Mitamura, K. Fukamichi, and K. Murata, J. Appl. Phys. **76**, 6682 (1994).

[31] W. Steiner, E. Gratz, H. Ortbauer, and H. W. Gamen, J. Phys. F: Met. Phys. **8**, 1525 (1978).

[32] E. Gratz, N. Pillmayr, E. Bauer, and G. Hilscher, J. Magn. Magn. Mater. **70**, 159 (1987).

[33] N. H. Duc, V. Sechovski, D. T. Hung, and N. H. K. Ngan, Physica B (Amsterdam) **179**, 111 (1992).

[34] N. H. Duc, P. E. Brommer, X. Li, F. R. de Boer, and J. J. M. Franse, Physica B (Amsterdam) **212**, 83 (1995).

[35] E. Gratz, R. Hauser, A. Lindbaum, M. Maikis, R. Resel, G. Schaudy, R. Z. Levitin, A. S. Markosyan, I. S. Dubenko, A. Yu. Sokolov, and S. W. Zochowski, J. Phys.: Condens. Matter **7**, 597 (1995).

[36] N. V. Baranov and A. N. Pirogov, J. Alloys Compd. **217**, 31 (1995).

[37] N. V. Baranov, A. A. Yermakov, and A. Podlesnyak, J. Phys.: Condens. Matter **15**, 5371 (2003).

[38] A. T. Burkov, A. Yu. Zyuzin, T. Nakama, and K. Yagasaki, Phys. Rev. B **69**, 144409 (2004).

[39] We measured resistivity of pure $R\mathrm{Co}_2$ compounds (except TmCo_2) using new samples, prepared according to the same procedure as the samples of $\mathrm{Ho}(\mathrm{Al}_x\mathrm{Co}_{1-x})$ alloys. These new results agree within experimental uncertainty with earlier data from Refs. 3 and 43.

[40] S. Khmelevskyi and P. Mohn, J. Phys.: Condens. Matter **12**, 9453 (2000).

[41] K. Ueda and T. Moriya, J. Phys. Soc. Jpn. **39**, 605 (1975).

[42] T. Moriya, in *Spin Fluctuations in Itinerant Electron Magnetism*, Springer Series in Solid State Sciences Vol. 56, edited by M. Cardona, P. Fulde, and H.-J. Quisser (Springer-Verlag, Berlin, 1985), Chap. 5.

[43] R. Hauser, E. Bauer, and E. Gratz, Phys. Rev. B **57**, 2904 (1998).

[44] T. Nakama, K. Shintani, K. Yagasaki, A. T. Burkov, and Y. Uwatoko, Phys. Rev. B **60**, 511 (1999).

[45] T. Nakama, K. Yagasaki, and A. T. Burkov (unpublished).

[46] R. D. Barnard, *Thermoelectricity in Metals and Alloys* (Tailor & Francis, London, 1972).